Available online at www.sciencedirect.com
ScienceDirect
Trans. Nonferrous Met. Soc. China 33(2023) 2064−2075
Transactions of Nonferrous Metals Society of China
www.tnmsc.cn

Effect of rolling temperature and reduction on brick-and-mortar Ti_2Ni/TiNi composite

Chen JIA[1], Zhi-ping XIONG[1,2], De-zhen YANG[1], Yang-wei WANG[1,2], Xing-wang CHENG[1,2]

1. National Key Laboratory of Science and Technology on Materials under Shock and Impact, Beijing Institute of Technology, Beijing 100081, China;
2. Tangshan Research Institute, Beijing Institute of Technology, Tangshan 063000, China

Received 14 February 2022; accepted 13 April 2022

Abstract: The brick-and-mortar Ti_2Ni/TiNi composite, composed of Ti_2Ni bricks distributed among TiNi mortars, was successfully produced by hot rolling laminated Ti_2Ni/TiNi composite. The rolling temperature and reduction have large effects on brick width and brick interspacing, respectively. When the compression is carried out perpendicular to the stacking direction, all the samples exhibit delamination fracture, which is harmful to mechanical performances. When loading is parallel to the stacking direction, too large brick width and too small brick interspacing both boost the delamination between brittle Ti_2Ni and ductile TiNi. After 60% rolling at 700 °C, the brick-and-mortar composite exhibits a largest strength of (1923.11±70.78) MPa and a largest fracture strain of 0.190±0.017 because suitable brick width and interspacing inhibit the delamination and promote crack deflection. Further optimization of mechanical properties can be achieved by the adjustment of brick width and interspacing.
Key words: brick-and-mortar structure; TiNi; delamination; rolling

1 Introduction

Laminated composite, made by alternatively stacking a brittle and a ductile constituent, has received much attention from engineering and scientific aspects due to its good combination of strength and ductility in comparison with a single brittle or ductile constituent [1−7]. For example, a Ti_2Ni/TiNi laminated composite has a compressive strength of (1774±15) MPa and a fracture strain of 0.15±0.01 [8]; whereas, a single Ti_2Ni exhibits crushing fracture and a single TiNi displays a large fracture strain of 0.40 but a much low strength of 700 MPa [9]. Various laminated composites have been developed, such as SiC/C [1], TiC/Ti [10], Ti_3Al/Ti [11], Al/Ni [12], Ti_2Ni/TiNi [13], Ni_2Al/Ni [14] and maraging steel/316L austenitic stainless steel [15]. This laminated structure, in fact, originates from the natural nacre consisting of aragonite platelets (brick) and protein (mortar) assembled in a brick-and-mortar way [16−22]. However, the laminated composite actually exhibits a layer-by-layer structure, indicating that further effort should be paid on the development of real brick-and-mortar structure.

The brick-and-mortar structure has been firstly attempted to develop by SELLINGER et al [23] using continuous self-assembly silica/poly(dodecyl methacrylate). However, this technique is restricted to the fabrication of thin films. Freeze casting [24−26] and co-extrusion [27−29] are two popular ways to fabricate bulky brick-and-mortar composite like Al_2O_3/PMMA (polymethyl

Corresponding author: Zhi-ping XIONG, Tel: +86-13126739386, E-mail: zpxiong@bit.edu.cn;
Xing-wang CHENG, E-mail: chengxw@bit.edu.cn
DOI: 10.1016/S1003-6326(23)66244-2
1003-6326/© 2023 The Nonferrous Metals Society of China. Published by Elsevier Ltd & Science Press

methacrylate) in a small-scale, which exhibits a double flexural strength compared to the corresponding laminated composite. However, the complicated procedures inhibit their mass production in industry. For example, freeze casting predominantly includes freezing, sintering and filling procedures, which require careful operation and complex instruments.

The present authors [8] have reported the successful fabrication of Ti_2Ni/TiNi brick-and-mortar composite by hot pressing and hot rolling, which has the potential to be capable of industrial production. However, how to tune the brick-and-mortar structure has not yet been investigated. WILKERSON et al [28] have reported that when decreasing the brick width from 430.7 to 186.4 μm in a Al_2O_3/Ni brick-and-mortar composite, the flexural strength increases from 110 to 158 MPa while the fracture toughness increases from 6.6 to 12.6 MPa·$m^{1/2}$. In the present study, the effect of rolling temperature and reduction on the microstructure evolution and mechanical performance has been systematically investigated in the Ti_2Ni/TiNi brick-and-mortar metallic composite. This study further proves the feasibility to fabricate different brick-and-mortar composites in mass production by hot rolling.

2 Experimental

2.1 Fabrication procedures

The Ti (0.020 mm) and Ni (0.045 mm) foils were firstly cut into 200 mm × 80 mm and ultrasonically cleaned in ethanol solution, then alternatively stacked and finally hot pressed. The temperature and pressure were controlled as illustrated in Fig. 1(a). The detailed procedures can be referred to Ref. [13]. As a result, Ti_2Ni/TiNi laminated composite was produced, where the light grey is TiNi and the dark grey is Ti_2Ni (Fig. 1(b)). The laminated composite was further hot-rolled at different temperatures (600, 700 and 800 °C) and at different reductions (30%, 60% and 70%). The nomenclature combines the temperature and reduction, such as 700−60 sample where 700 indicates the rolling temperature of 700 °C and 60 suggests the rolling reduction of 60%.

2.2 Microstructure and mechanical property characterization

The samples (2 mm × 3 mm × 4 mm) were cut from the rolled specimens, mechanically polished but not etched. The cross-sections of rolling-direction and transverse-direction, transverse-direction and normal direction, rolling-direction and normal-directions are all characterized and assembled. The microstructures were characterized using a Zeiss Supra 55 scanning electron microscope (SEM) in back-scattering (BS) mode.

The cylinder samples (*d*4 mm × 6 mm) for uniaxial compression were cut both parallel and perpendicular to the stacking direction (Fig. 2). The top and bottom were both polished in order to remove the oxidation and keep parallel. The uniaxial compression was carried out using an electronic universal testing machine at an initial strain rate of 1×10^{-4} s^{-1}.

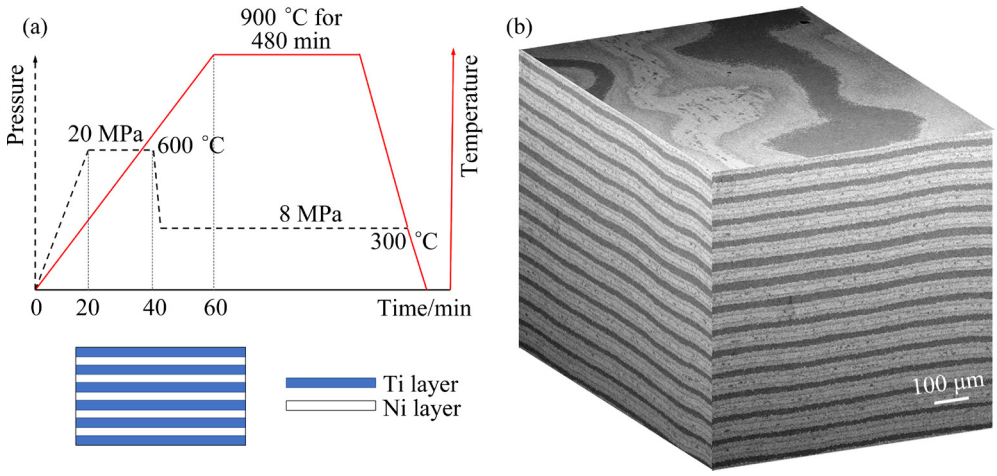

Fig. 1 Schematic of stacking and hot-pressing (a) and microstructure of Ti_2Ni/TiNi laminated composite (b)

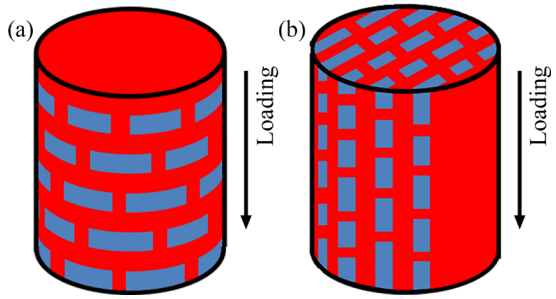

Fig. 2 Uniaxial compression parallel (a) and perpendicular (b) to stacking direction

3 Results

3.1 Effect of rolling temperature

3.1.1 Effect of rolling temperature on microstructure

Figure 3 shows the three-dimensional microstructures after rolling by 60% at different temperatures. The light grey is TiNi phase while the dark grey is Ti_2Ni phase in the SEM-BSE mode. When rolling at 600 °C, the laminated Ti_2Ni layers in the laminated composite (Fig. 1) are broken. As a result, the normal−rolling cross-section exhibits a brick-and-mortar structure. Namely, the TiNi mortar is continuous, among which the Ti_2Ni brick is distributed in a brick-and-mortar way. The normal−transverse cross-section also displays the broken TiNi phase distributed among the TiNi mortar, but the brick is not homogeneous compared to the normal−rolling cross-section. Here, the rolling−normal microstructure is carefully analyzed. As can be seen in Fig. 3(a), the interface parallel to the rolling direction between TiNi and Ti_2Ni is clear and well bonded; whereas, the voids are observed along the interface perpendicular to the rolling direction.

With decreasing rolling temperature from 800 to 600 °C, the brick width significantly decreases from (87.73±45.35) to (28.18±9.85) μm, the brick thickness moderately decreases from (18.27±2.51) to (12.35±2.19) μm, and the interspacing between neighboring bricks in the rolling direction moderately decreases from (46.94±24.94) to (28.86±13.64) μm (Table 1). All these suggest that the Ti_2Ni layer in the laminated composite (Fig. 1) is broken more seriously when the rolling temperature is decreased. As a result, number of Ti_2Ni brick increases (Fig. 3) and thus, the rolling temperature has a large impact on the brick width. However, decreasing rolling temperature from 800 to 600 °C introduces more voids along the interface between TiNi and Ti_2Ni, leading to an increase in the void density from (161±29) to (729±92) mm^{-2}. When rolling at 800 °C, the width of Ti_2Ni brick deviates from the rolling direction (Fig. 3(c)); decreasing rolling temperature down to 600 °C, the width of Ti_2Ni brick becomes along the rolling direction (Fig. 3(a)).

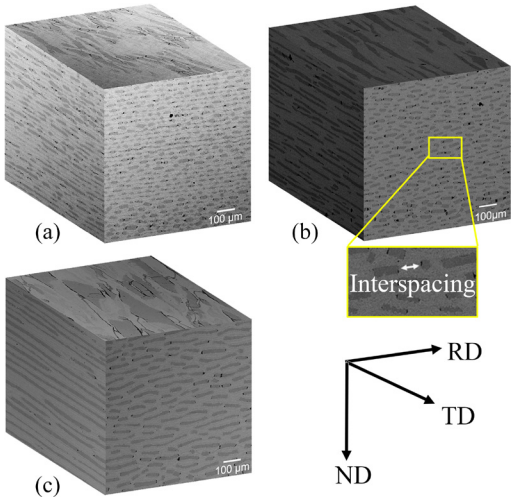

Fig. 3 Three-dimensional SEM images after hot rolling by 60% reduction at different temperatures: (a) 600 °C; (b) 700 °C; (c) 800 °C

3.1.2 Effect of rolling temperature on mechanical properties

Figures 4(a, b) shows compressive engineering stress−engineering strain curves after 60% rolling at different temperatures when deformed parallel and perpendicular to the stacking direction. All

Table 1 Statistical analysis of microstructural characteristics after rolling by 60% reduction at different temperatures (At least five SEM-BSE images are analyzed for each condition using Image J software)

Rolling temperature/°C	Brick thickness/μm	Brick width/μm	Width/thickness	Interspacing/μm	Void density/mm^{-2}
600	12.35±2.19	28.18±9.85	2.28	28.86±13.64	729±92
700	14.07±2.40	37.28±12.17	2.65	38.79±14.75	629±106
800	18.27±2.51	87.73±45.35	4.80	46.94±24.94	161±29

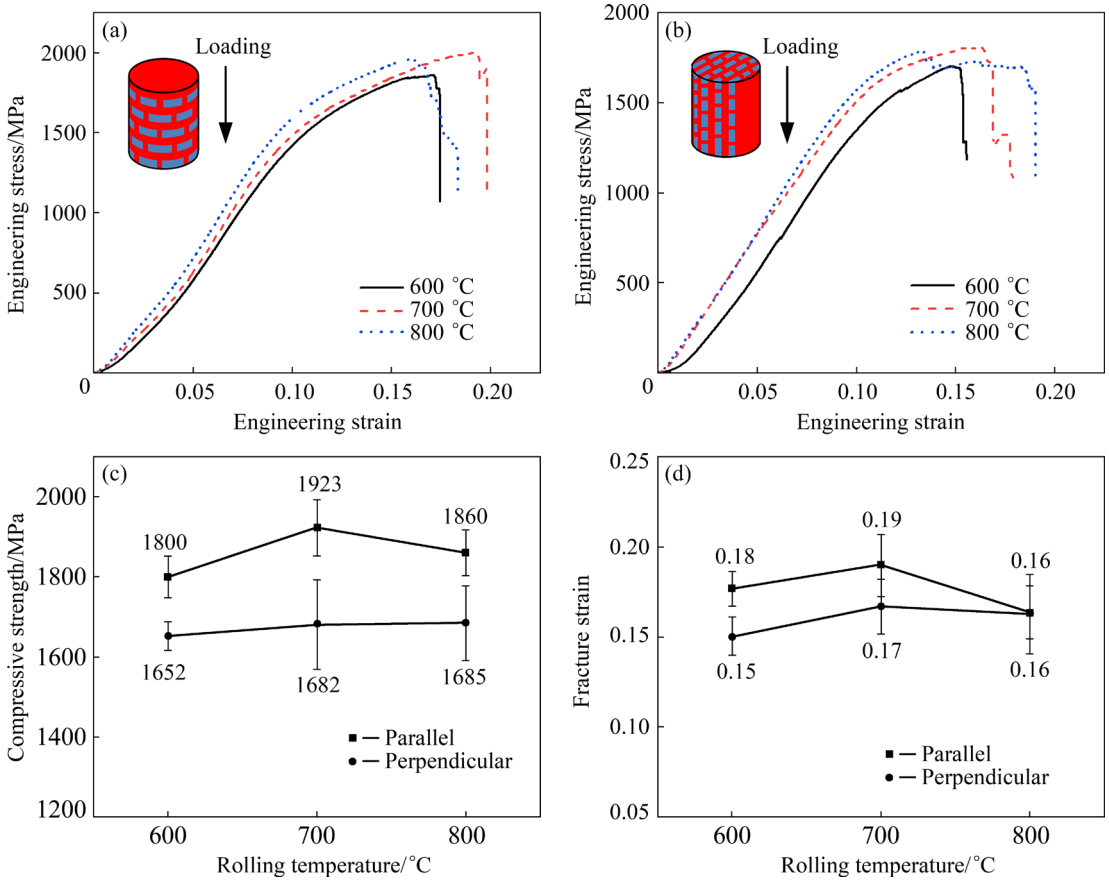

Fig. 4 Uniaxial compression test results after hot rolling by 60% reduction at 600, 700 and 800 °C: (a, b) Compressive engineering stress−engineering strain curves after loading parallel (a) and perpendicular (b) to stacking direction; (c, d) Evolution of compressive strength (c) and fracture strain (d) with rolling temperature

these curves exhibit the similar shape of a spoon, indicating the similar deformation mechanism. This is because all the samples consist of the same fractions of TiNi and Ti_2Ni phases. However, the distribution of Ti_2Ni bricks is different and it affects the mechanical response during uniaxial compression. After rolling at 700 °C, the 700-60 sample displays the largest strength and ductility during parallel and perpendicular compression; exceptionally, the 700-60 sample exhibits a similar compressive strength to the 800-60 sample during perpendicular compression. When increasing or decreasing rolling temperature, the strength and ductility are both decreased (Figs. 4(c, d)).

Figure 5 shows the crack propagation during the uniaxial compression parallel to the stacking direction. After rolling at 600 °C, the 600-60 sample exhibits a main crack 45° deviated from the compression direction, which is generally straight with few deflections (Fig. 5(a)). This straight main crack is formed due to a small brick width of (28.18±9.85) μm and in turn, a small crack deflection. After rolling at 700 °C, a 45° main crack also induces the fracture, but it is not straight and many defections can be observed (Fig. 5(c)). Based on the short fiber reinforcement [30], a larger brick width of (37.28±12.17) μm in the 700-60 sample can sustain more load than the 600-60 sample having a brick width of (28.18±13.64) μm. This can delay the fracture, leading to both larger compressive strength and ductility in the 700-60 sample. In addition, many cracks are formed inside the Ti_2Ni brick and their propagation is inhibited by the TiNi matrix (Fig. 5(d) vs Fig. 5(b)). However, further increasing the brick width in the 800-60 sample ((87.73±45.35) μm) boosts the crack propagation along the interface between TiNi and Ti_2Ni, resulting in the delamination. This delamination makes parts of the sample shatter and thus, the forced area is reduced and the stress is increased, which boots the formation of a straight 45° main crack (Figs. 5(e, f)). As a result, the strength and ductility are simultaneously decreased (Figs. 4(c, d)).

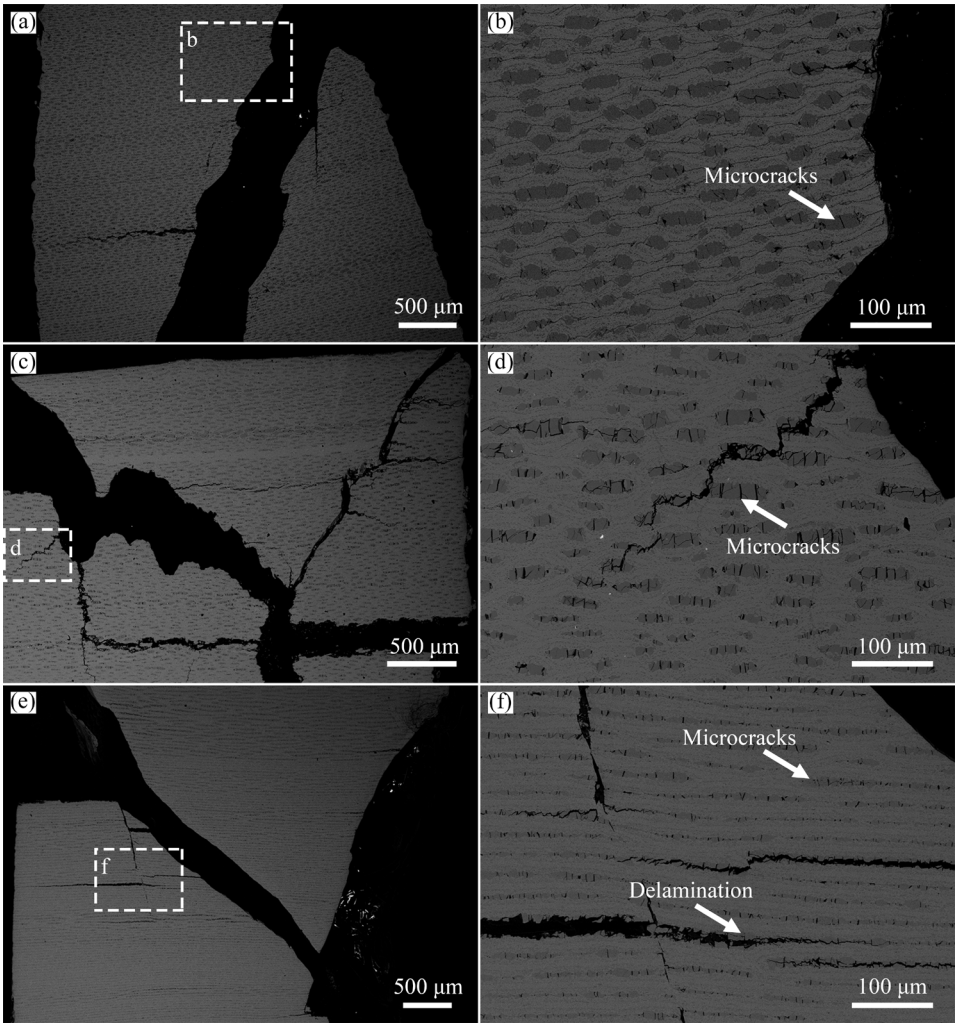

Fig. 5 Crack propagation after rolling by 60% reduction at 600 °C (a, b), 700 °C (c, d) and 800 °C (e, f) with uniaxial compression parallel to stacking direction

Figure 6 shows the crack propagation after deformation perpendicular to the stacking direction. All the samples are fractured by delamination, which boosts the catastrophe [8,31]. As a result, the compressive strength fluctuates around 1600 MPa while the fracture strain fluctuates around 0.16 (Figs. 4(c, d)). Noticeably, this delamination failure is similar to the laminated composite [31,32], but totally different from the rupture when deformed parallel to the stacking direction (Fig. 5 vs Fig. 6). As a result, the strength and ductility after perpendicular compression are both smaller than those after parallel compression (Figs. 4(c, d)).

3.2 Effect of rolling reduction

3.2.1 Effect of rolling reduction on microstructure

According to the above analysis of mechanical behaviors, the deformation temperature of 700 °C is selected. Similar to the microstructures after rolling at different temperatures (Fig. 3), after rolling at different reductions, Fig. 7 also shows the brick-and-mortar structures where dark grey Ti_2Ni bricks homogenously distribute among the light grey TiNi mortars. When rolling at a reduction of 30%, many voids (629 mm^{-2}) are formed at the interface perpendicular to the rolling direction (Fig. 7(a)). Increasing the rolling reduction can eliminate the voids by the flow of soft TiNi phase, leading to a decrease in the void density from (686±17) to (141±48) mm^{-2} (Table 2).

Increasing the rolling reduction from 30% to 60%, the width of Ti_2Ni brick moderately decreases from (48.14±21.07) to (33.52±13.48) μm, the thickness of Ti_2Ni brick moderately decreases from (17.72±1.70) to (13.35±3.40) μm and correspondingly, the interspacing between Ti_2Ni bricks along the rolling direction significantly increases from (22.55±7.69) to (42.14±18.27) μm

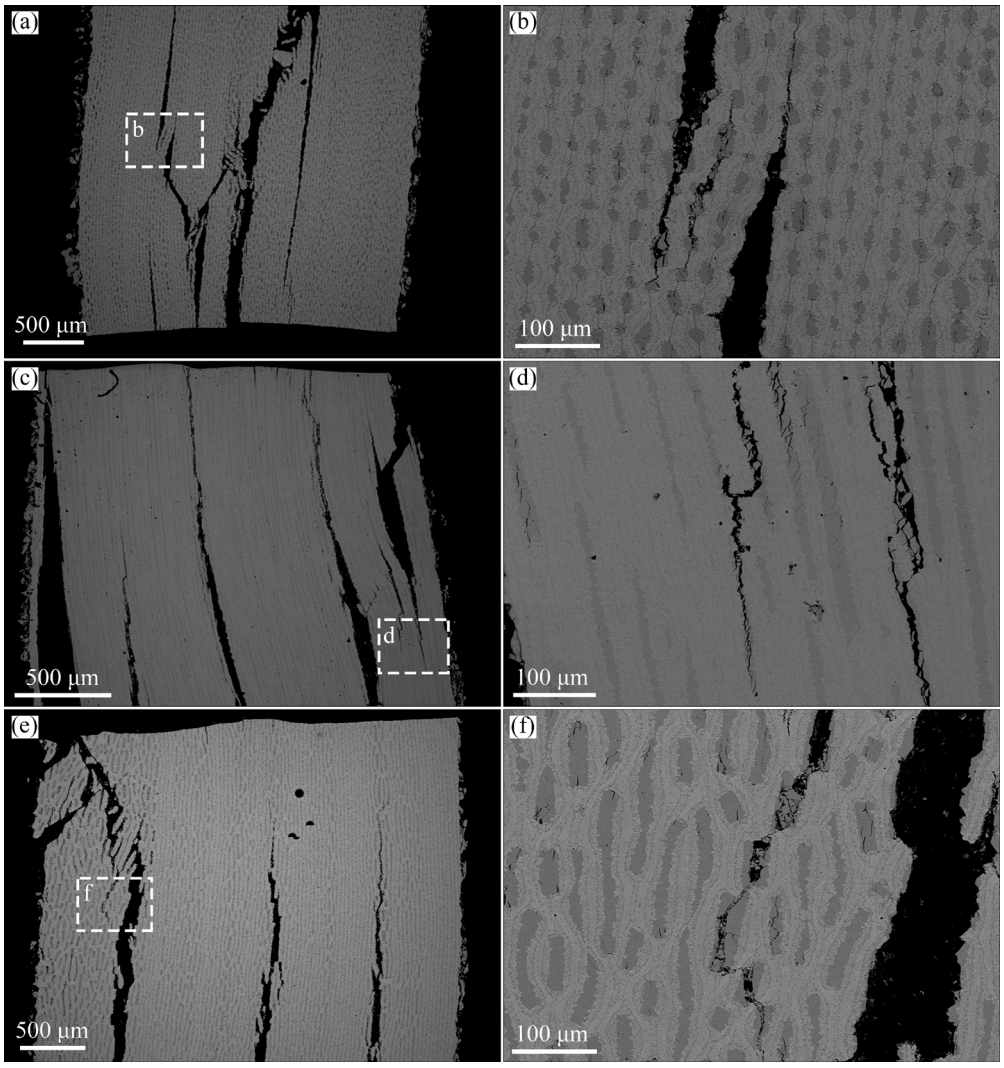

Fig. 6 Crack propagation after rolling by 60% reduction at 600 °C (a, b), 700 °C (c, d) and 800 °C (e, f) with uniaxial compression perpendicular to stacking direction

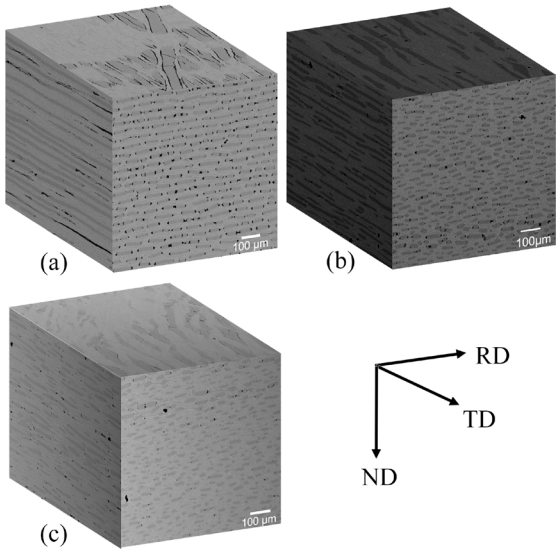

Fig. 7 Three-dimensional SEM images after 700 °C hot rolling at reductions of 30% (a), 60% (b) and 70% (c)

(Table 2). All these suggest that the Ti_2Ni layer in the laminated composite (Fig. 1) is broken more seriously when increasing the rolling reduction. As can be concluded, the rolling reduction has a large influence on the brick interspacing. Additionally, increasing rolling reduction makes the brick deviate from the rolling direction (Fig. 7(a) vs Fig. 7(c)).

3.2.2 Effect of rolling reduction on mechanical properties

Similar to the samples after rolling by 60% at different temperatures, the samples after 700 °C rolling at different reductions also exhibit a spoon shape of compressive engineering strain−engineering stress curves. This suggests that all the brick-and-mortar Ti_2Ni/TiNi samples have similar deformation mechanisms and the difference in deformation behavior is induced by the brick Ti_2Ni

distribution. After rolling at a reduction of 60%, the 700-60 sample has the largest strength and fracture strain after both parallel and perpendicular compression.

Figures 8(a, b) show the compressive engineering stress−engineering strain curves after rolling at 700 °C by different reductions. Figure 9 shows the crack propagation after deformation parallel to the stacking direction after 700 °C rolling by different reductions. After rolling at a reduction of 30%, the 700-30 sample exhibits a straight main crack which deviates 45° from the compression direction (Fig. 9(a)), leading to the lowest compressive strength and fracture strain (Figs. 8(c, d)). This main crack is formed due to a small brick interspacing of (22.55±7.69) μm and, in turn, the sample shatter by easy delamination (Fig. 9(b)). Increasing rolling reduction increases the brick interspacing and this can increase the crack deflection during its propagation in the TiNi matrix, resulting in the formation of a deflected main crack (Fig. 9(c)). This delays the sample fracture and increases both strength and ductility in the 700-60 sample. However, further increasing the rolling reduction up to 70% increases the brick interspacing up to (42.14±18.27) μm. This large interspacing can fully inhibit the delamination and deflection, and thus, boost the 45° main crack formation (Fig. 9(e)), leading to a decrease in the both strength and ductility (Figs. 8(c, d)).

Table 2 Statistical analysis of microstructural characteristics after rolling at 700 °C by different reductions (At least five SEM-BSE images are analyzed for each condition using Image J software)

Rolling reduction/%	Brick thickness/μm	Brick width/μm	Width/Thickness	Interspacing/μm	Void density/mm^{-2}
30	17.72±1.70	48.14±21.07	2.80	22.55±7.69	686±17
60	14.07±2.40	37.28±12.17	2.65	38.79±14.75	629±106
70	13.35±3.40	33.52±13.48	2.51	42.14±18.27	141±48

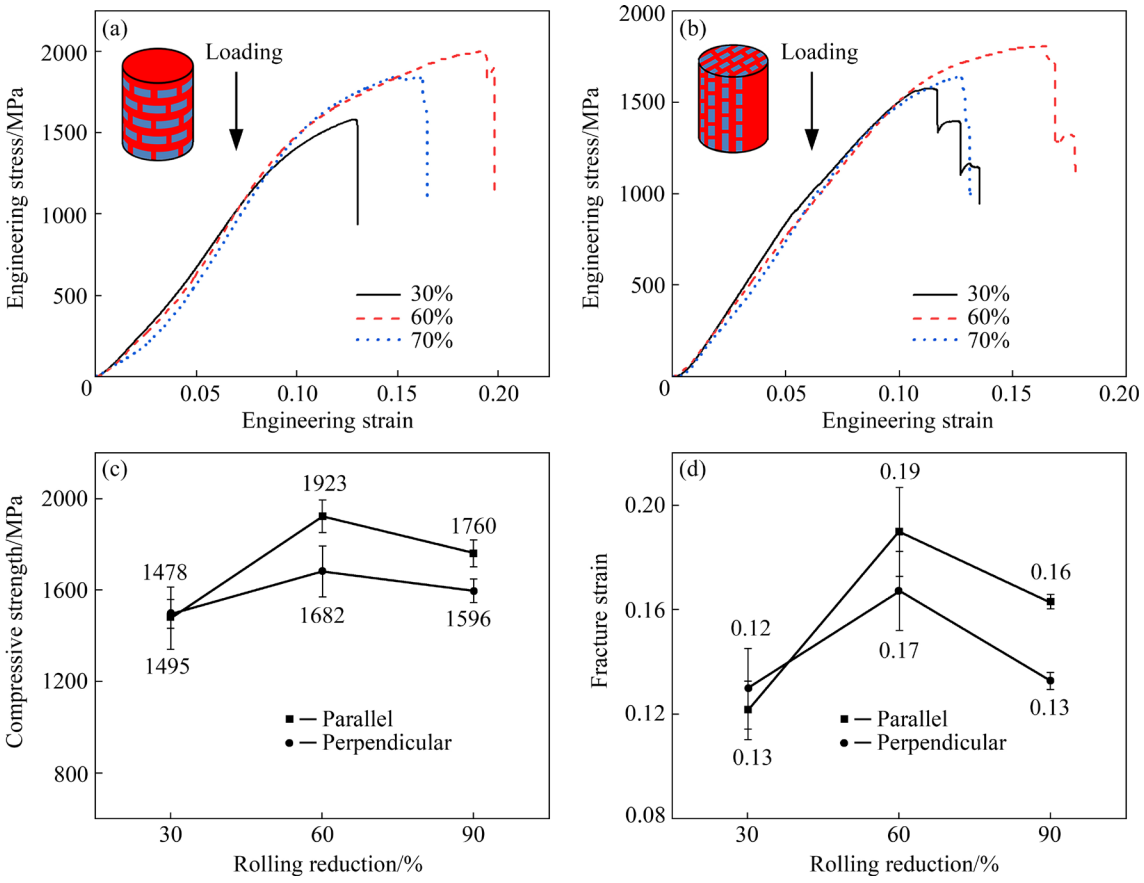

Fig. 8 Uniaxial compression test results after hot rolling at 700 °C by reductions of 30%, 60% and 70%: (a, b) Compressive engineering stress−engineering strain curves after loading parallel (a) and perpendicular (b) to stacking direction; (c, d) Evolution of compressive strength (c) and fracture strain (d) with rolling reduction

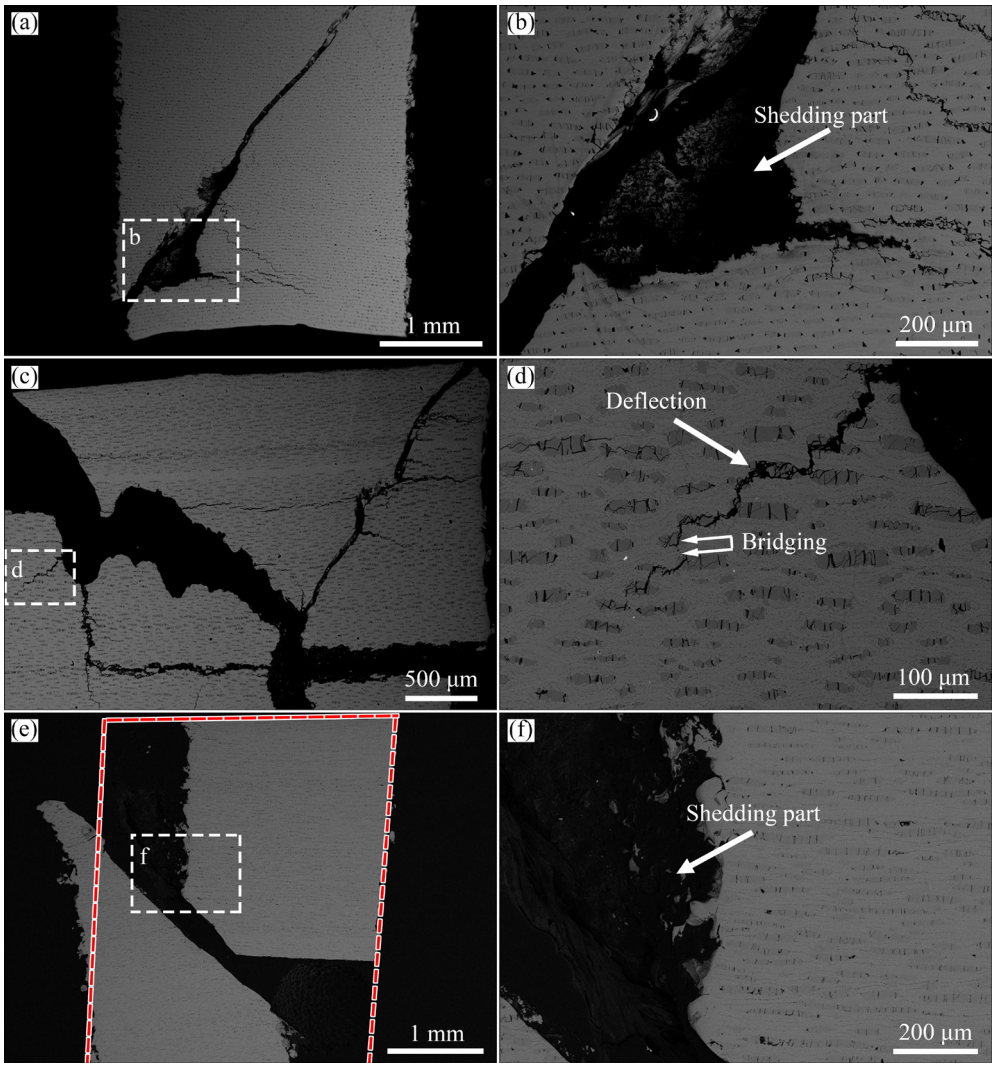

Fig. 9 Crack propagation with uniaxial compression parallel to stacking direction after hot rolling at 700 °C by reduction of 30% (a, b), 60% (c, d) and 70% (e, f)

Figure 10 shows the crack propagation when deformed perpendicular to the stacking direction after 700 °C rolling by different reductions. After rolling at a reduction of 30%, the brick interspacing is only (22.55±7.69) μm, leading to the flexure (Fig. 10(a)) similar to laminated composite [8,32]. Increasing rolling reduction increases the brick interspacing and avoids flexure, which increases the ductility and strength. But still, the delamination between TiNi and Ti_2Ni occurs (Figs. 10(c, d)). This delamination is the reason why the strength and ductility when deformed perpendicular to the stacking direction are lower than those when deformed parallel to stack direction (Figs. 8(c, d)). Unexpectedly, a large brick interspacing ((42.14± 18.27) μm) after rolling at a reduction of 70% leads to an early fracture and a corresponding small strength. This is probably because TiNi burdens a large plastic deformation (can be seen in Fig. 10(f)), leading to Ti_2Ni rotation and easy crack connection.

4 Discussion

The brick-and-mortar structure has been successfully produced in the present investigation by hot rolling Ti_2Ni/TiNi laminated composite and this Ti_2Ni/TiNi laminated composite is fabricated using hot pressing. Due to the usage of hot pressing and hot rolling, a large-scale sample has been produced up to 200 mm × 80 mm × 6 mm in the laboratory and these procedures can be easily scaled in the industry for mass production. Contrarily, only small size samples (like 25 mm × 10 mm × 10 mm)

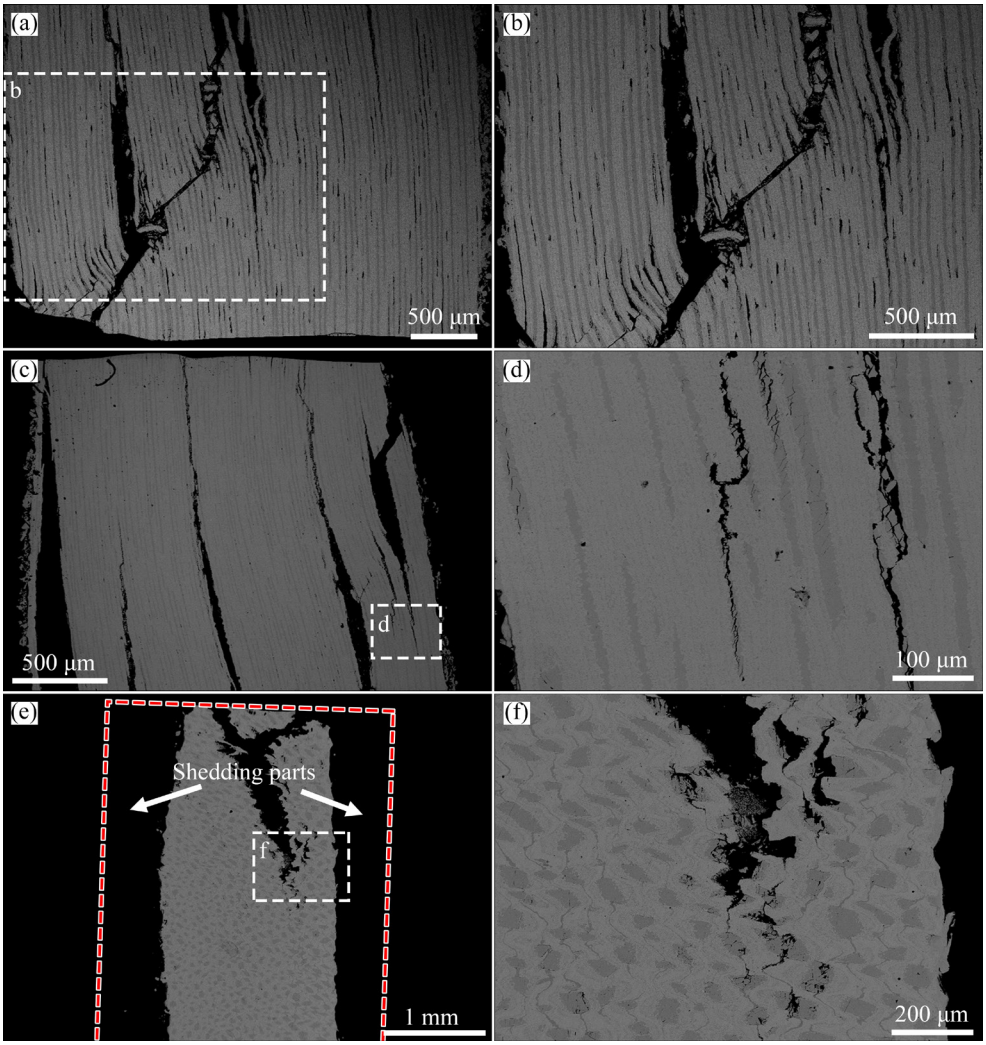

Fig. 10 Crack propagation with uniaxial compression perpendicular to stacking direction after hot rolling at 700 °C by reduction of 30% (a, b), 60% (c, d) and 70% (e, f)

can be produced using freeze casting [25] or co-extrusion [27]. In addition, these two methods have very complicated procedures, which are not suitable for mass production in industry; for example, co-extrusion needs a long-time for tube-shaped materials preparation, such as extrusion, cutting, stacking and sintering [27].

In addition, it is easy to tune the micro-structures of the brick-and-mortar Ti_2Ni/TiNi intermetallic composite by the adjustment of rolling temperature (Fig. 3) and rolling reduction (Fig. 7). As illustrated in Fig. 11, when laminated composite is deformed, cracks are formed in the brittle Ti_2Ni layer due to its intrinsic brittleness [32]. Decreasing temperature makes more cracks formed in the Ti_2Ni layer, leading to a decrease in the Ti_2Ni brick width. This is because a higher temperature can boost the co-deformation between ductile TiNi and brittle Ti_2Ni and as a result, less cracks are formed in the Ti_2Ni layer. Thus, rolling temperature has a large effect on the Ti_2Ni brick width (Table 1) by affecting the crack formation in the brittle Ti_2Ni layer. Following the crack formation, the TiNi matrix fills in the cracks under the plastic deformation (Fig. 11). Increasing rolling reduction enhances the plastic deformation of ductile TiNi matrix, leading to an increase in the brick interspacing along the rolling direction (Table 2) by filling more TiNi into the cracks. Therefore, the rolling reduction has a significant influence on the brick interspacing by affecting the plastic deformation in the TiNi matrix.

The mechanical behaviors are affected by the deformation mode [33], which is determined by the structure of Ti_2Ni/TiNi brick-and-mortar composite. When deformed perpendicular to the stacking

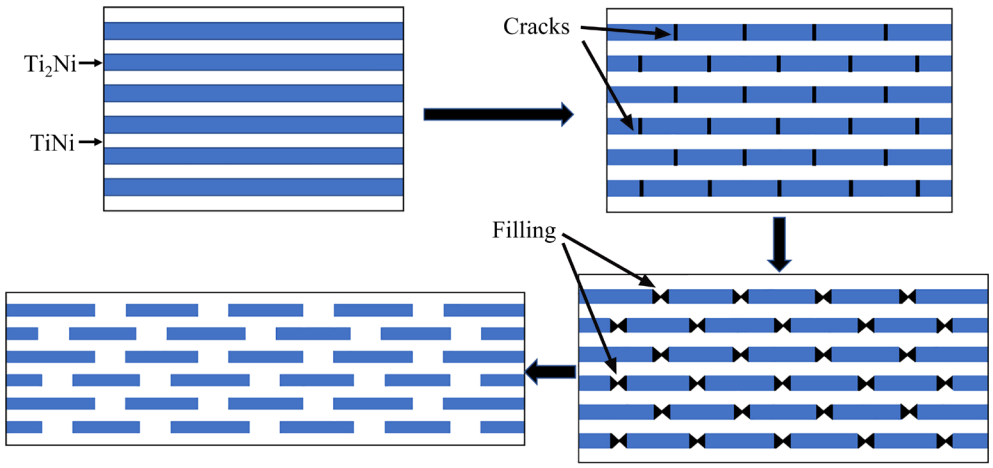

Fig. 11 Schematic diagram of brick-and-mortar formation

direction, the delamination between brittle Ti_2Ni and ductile TiNi is the main failure way (Figs. 6 and 10), which deteriorates the mechanical properties. Thus, the mechanical behavior is significantly concerned when the loading direction is parallel to the stacking direction. The cracks prefer to nucleate and propagate along the interfaces between ductile TiNi and brittle Ti_2Ni due to uncoordinated deformation resulting from their different strengths. Similar phenomenon has been reported in the TiC/Ti [34], Ti_2Ni/TiNi [31] and Al_3Ti/Ti [32] laminated composites. Therefore, the brick width is a much more important parameter than the brick thickness. The 800-60 sample has a pretty large brick width of (87.73±45.35) μm, which boots the formation of long cracks along the brick width during the deformation. This promotes the delamination along the previous Ti_2Ni layer before hot rolling (Fig. 5(f)), leading to the occurrence of fragment from the whole sample. In turn, the forced area is reduced and the stress is increased, which accelerates the fracture by the formation of 45° main crack (Fig. 5(e)). However, the brick width also cannot be too small. The 600-60 sample has a too small width of (28.86±13.64) μm to lose the advantage of brick-and-mortar structure; instead, it is fractured in a way of 45° shear failure, which is similar to the single constituent [35]. Despite the brick width, the brick interspacing is another important structural parameter. The 700-30 sample has a small brick interspacing of (22.55±7.69) μm, which boosts the crack connection between the neighboring cracks in the rolling direction. This leads to the early delamination and the fragment of the sample (Fig. 9(b)).

It can be concluded here that the key point is to avoid the delamination fracture in the brick-and-mortar composite by the adjustment of brick width and interspacing. The avoidance of the full delamination can delay the fracture by the crack formation in the brick Ti_2Ni, the crack deflection, the crack bridging and intermittent delamination (Figs. 5 and 9). Too large width can promote the delamination due to the crack nucleation and propagation along the width (namely interface between the ductile TiNi and brick Ti_2Ni). Too small brick interspacing can also boost the delamination because the cracks in the neighboring bricks can be connected by the fracture process zones ahead of the cracks [36]. Thus, the strength does not have a clear relationship with either the brick width (Fig. 12(a)) or the brick interspacing (Fig. 12(b)).

5 Conclusions

(1) The microstructural characteristics can be tuned by rolling temperature and rolling reduction, which have large effects on brick width and brick interspacing, respectively.

(2) When deformed perpendicular to the stacking direction, the delamination fracture is predominant and it deteriorates the mechanical performance. Instead, loading parallel to the stacking direction is concerned for application.

(3) The way to improve the mechanical properties during parallel loading is to avoid the delamination by adjustment of brick width and brick interspacing. Too large Ti_2Ni brick width and too small Ti_2Ni brick interspacing both can boost

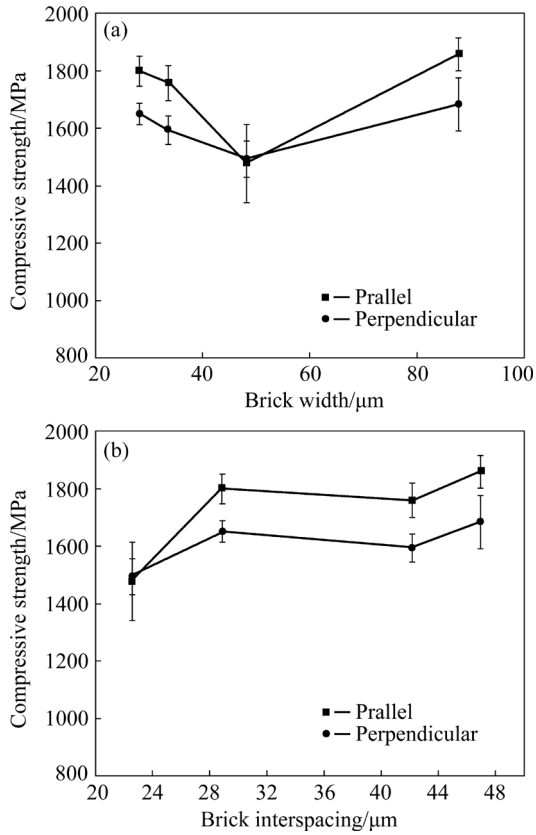

Fig. 12 Evolution of mechanical properties with brick width (a) and interspacing (b)

the delamination. After 60% rolling at 700 °C, the largest compressive strength of (1923.11± 70.78) MPa and the largest fracture strain of (0.190±0.017) are achieved. Further optimization of mechanical properties can be realized through the design of brick-and-mortar structure using finite-element simulation.

Acknowledgments

The authors are grateful for the financial supports from the Beijing Institute of Technology Research Fund Program for Young Scholars, China (No. XSQD-201808006).

References

[1] CLEGG W J, KENDALL K, ALFORD N M, BUTTON T W, BIRCHALL J D. A simple way to make tough ceramics [J]. Nature, 1990, 347: 455−457.

[2] NIE Hui-hui, ZHANG Liu-wei, KANG Xiao-ping, HAO Xin-wei, LI Xian-rong, LIANG Wei. In-situ investigation of deformation behavior and fracture forms of Ti/Al/Mg/Al/Ti laminates [J]. Transactions of Nonferrous Metals Society of China, 2021, 31(6): 1656−1664.

[3] MIZUUCHI K, INOUE K, SUGIOKA M, ITAMI M, LEE J H, KAWAHARA M. Properties of Ni-aluminides-reinforced Ni-matrix laminates synthesized by pulsed-current hot pressing (PCHP) [J]. Materials Science and Engineering A, 2006, 428: 169−174.

[4] CHENG Wen-juan, LIU Yong, ZHAO Da-peng, LIU Bin, TAN Yan-ni, WANG Xiao-gang, TANG Han-chun. Crack propagation behavior of inhomogeneous laminated Ti−Nb metal−metal composite [J]. Transactions of Nonferrous Metals Society of China, 2019, 29(9): 1882−1888.

[5] DUREJKO T, LIPINSKI S, BOJAR Z, BYSTRZYCKI J. Processing and characterization of graded metal/intermetallic materials: The example of Fe/FeAl intermetallics [J]. Materials & Design, 2011, 32: 2827−2834.

[6] BATAEV I A, BATAEV A A, MALI V I, PAVLIUKOVA D V. Structural and mechanical properties of metallic–intermetallic laminate composites produced by explosive welding and annealing [J]. Materials & Design, 2012, 35: 225−234.

[7] LAUNEY M E, MUNCH E, ALSEM D H, SAIZ E, TOMSIA A P, RITCHIE R O. A novel biomimetic approach to the design of high-performance ceramic–metal composites [J]. Journal of the Royal Society Interface, 2010, 7(46): 741−753.

[8] JIA Chen, XIONG Zhi-ping, MU Guang-yi, CHENG Zhi-fang, WANG Yang-wei, CHENG Xing-wang. Simultaneously improved strength and toughness of hot-rolled brick-and-mortar TiNi/Ti_2Ni intermetallic composite [J]. Materials Science and Engineering A, 2021, 815: 141302.

[9] ISHIDA A, SATO M, MIYAZAKI S. Mechanical properties of Ti–Ni shape memory thin films formed by sputtering [J]. Materials Science and Engineering A, 1999, 273/274/275: 754−757.

[10] TAN You-de, CAI Hong-nian, CHENG Xing-wang, MA Zhao-long, XU Zi-qi, ZHOU Zhi-fang. Microstructural and mechanical properties of in-situ micro-laminated TiC/Ti composite synthesised [J]. Materials Letters, 2018, 228: 1−4.

[11] ZHANG Jian-yu, WANG Yan-hui, ZHANG Lv, CHEN Qing-an, CHEN Ya-yu, LI He-zong. Formation mechanism and growth kinetics of $TiAl_3$ phase in cold-rolled Ti/Al laminated composites during annealing [J]. Transactions of Nonferrous Metals Society of China, 2022, 32(2): 524−539.

[12] ZHU Hui-wen, YU Bao-yi, ZHANG Hao, YU Bo-ning, LV Shu-ning, ZHENG Li, LI Run-xia. Effect of annealing treatment on microstructure and mechanical properties of Al/Ni multilayer composites during accumulative roll bonding (ARB) process [J]. Journal of Iron Steel Research International, 2020, 27: 96−104.

[13] ZHANG You-jing, CHENG Xing-wang, CAI Hong-nian. Fabrication, characterization and tensile property of a novel Ti_2Ni/TiNi micro-laminated composite [J]. Materials & Design, 2016, 92: 486−493.

[14] XIA Zhen-hai, LIU Jin-hai, ZHU Shu-qing, ZHAO Ya-zhong. Fabrication of laminated metal–intermetallic composites by interlayer in-situ reaction [J]. Journal of Materials Science, 1999, 34(15): 3731−3735.

[15] ZHANG Le, WANG Wei, SHAHZAD M B, SHAN Yi-yin, YANG Ke. A novel laminated metal composite with superior interfacial bonding composed of ultrahigh-strength maraging steel and 316L stainless steel [J]. Journal of Iron Steel Research International, 2020, 27: 433−439.

[16] WEGST U G K, BAI Hao, SAIZ E, TOMSIA A P, RITCHIE R O. Bioinspired structural materials [J]. Nature Materials, 2015, 14: 23−36.

[17] MEYERS M A, LIN Yun-min, CHEN Po-yu, MUYCO J. Mechanical strength of abalone nacre: Role of the soft organic layer, Journal of the Mechanical Behavior of Biomedical [J]. Materials, 2008, 1(1): 76−85.
[18] LIN Yu-min, MEYERS M A. Interfacial shear strength in abalone nacre [J]. Journal of the Mechanical Behavior of Biomedical Materials, 2009, 2(6): 607−612.
[19] EVANS A G, SUO Z, WANG R Z, AKSAY I A, HE M Y, HUTCHINSON J W. Model for the robust mechanical behavior of nacre [J]. Journal of Materials Research, 2001, 16(9): 2475−2484.
[20] BARTHELAT F, TANG H, ZAVATTIERI P D, LI C M, ESPINPSA H D. On the mechanics of mother-of-pearl: A key feature in the material hierarchical structure [J]. Journal of the Mechanics and Physics of Solids, 2007, 55(2): 306−337.
[21] YUE Shao, ZHAO Hong-ping, FENG Xi-qiao. On flaw tolerance of nacre: A theoretical study [J]. Journal of the Royal Society Interface, 2014, 11(92): 20131016.
[22] ESPINOSA H D, RIM J E, BARTHELAT F, BUEHLER M J. Merger of structure and material in nacre and bone-Perspectives on de novo biomimetic materials [J]. Progress in Materials Science, 2009, 54(8): 1059−1100.
[23] SELLINGER A, WEISS P M, NGUYEN A, LU Yun-feng, ASSINK R A, GONG Wei-liang, BRINKER C J. Continuous self-assembly of organic-inorganic nanocomposite coatings that mimic nacre [J]. Nature, 1998, 394: 256−260.
[24] MUNCH E, LAUNEY M E, ALSEM D H, SAIZ E, TOMSIA A P, RITCHIE R O. Tough, bio-inspired hybrid materials [J]. Science, 2008, 322(5907): 1516−1520.
[25] LAUNEY M E, MUNCH E, ALSEM D H, BARTH H B, SAIZ E, TOMSIA A P, RITCHIE R O. Designing highly toughened hybrid composites through nature-inspired hierarchical complexity [J]. Acta Materialia, 2009, 57: 2919−2932.
[26] DEVILLE S, SAIZ E, NALLA R, TOMSIA A. Freezing as a path to build complex composites [J]. Science, 2006, 311(5760): 515−518.
[27] WILKERSON R P, GLUDOVATZ B, WATTS J, TOMSIA A P, HILMAS G E, RITCHIE R O. A novel approach to developing biomimetic “nacre-like” metal-compliant-phase (nickel−alumina) ceramics through coextrusion [J]. Advanced Materials, 2016, 28(45): 10061−10067.
[28] WILKERSON R P, GLUDOVATZ B, WATTS J, TOMSIA A P, HILMAS G E, RITCHIE R O. A study of size effects in bioinspired, “nacre-like”, metal-compliant-phase (nickel−alumina) coextruded ceramics [J]. Acta Materialia, 2018, 148: 147−155.
[29] WILKERSON R P, GLUDOVATZ B, ELL J, WATTS J, HILMAS G E, RITCHIE R O. High-temperature damage-tolerance of coextruded, bioinspired (“nacre-like”), alumina/nickel compliant-phase ceramics [J]. Scripta Materialia, 2019, 158: 110−115.
[30] CHRISTENSEN R M. Mechanical properties of composite materials [J]. Mechanics of Composite Materials, 1983: 1−16.
[31] ZHANG You-jing, CHENG Xing-wang, CAI Hong-nian, ZHOU Ssi-meng, WANG Pei, YIN Jia-ming. The effects of thickness of original Ti foils on the microstructures and mechanical properties of Ti_2Ni/TiNi laminated composites [J]. Materials Science and Engineering A, 2017, 684: 292−302.
[32] PRICE R D, JIANG Feng-chun, KULIN R M, VECCHIO K S. Effects of ductile phase volume fraction on the mechanical properties of Ti−Al_3Ti metal-intermetallic laminate (MIL) composites [J]. Materials Science and Engineering A, 2011, 528: 3134−3146.
[33] ZHAO Lv, DING Li-peng, SOETE J, IDRISSI H, KERCKHOFS G, SIMAR A. Fostering crack deviation via local internal stresses in Al/NiTi composites and its correlation with fracture toughness [J]. Composites Part A: Applied Science and Manufacturing, 2019, 126: 105617.
[34] TAN You-de, XU Ling-yu, XU Zi-qi, ALI T, MA Zhao-long, CHENG Xing-wang, CAI Hong-nian. Effects of Ti foil thickness on microstructures and mechanical properties of in situ synthesized micro-laminated TiC/Ti composites [J]. Materials Science and Engineering A, 2019, 767: 138296.
[35] LUNG C W, MARCH N H. Mechanical properties of metals: Atomistic and fractal continuum approaches [M]. Singapore: World Scientific, 1999.
[36] ANDERSON T L. Fracture mechanics: Fundamentals and applications [M]. 3rd ed. Boca Raton: CRC Press, 1991.

轧制温度和压下量对 Ti_2Ni/TiNi 砖砌复合材料的影响

贾 晨[1]，熊志平[1,2]，杨德振[1]，王扬卫[1,2]，程兴旺[1,2]

1. 北京理工大学 冲击环境材料技术国家级重点实验室，北京 100081；
2. 北京理工大学 唐山研究院，唐山 063000

摘 要：Ti_2Ni/TiNi 砖砌复合材料由 TiNi 水泥和分布在其中的 Ti_2Ni 砖块组成，可以通过热轧 Ti_2Ni/TiNi 叠层复合材料进行制备。轧制温度和压下量分别对砖块宽度和间距有重要的影响。当压缩方向垂直于堆叠方向时，所有的样品均出现分层断裂，力学性能大幅降低。当压缩方向平行于堆叠方向时，太大的砖块宽度和太小的砖块间距都会促进 Ti_2Ni 和 TiNi 之间发生分层的现象。在 700 ℃进行压下量为 60%的轧制，砖砌复合材料得到最高的强度((1923.11±70.78) MPa)和最大的断裂应变(0.190±0.017)，这是由于合适的砖块宽度和间距阻碍分层失效并促进裂纹的偏转。由此可见，通过优化砖块宽度和间距，可以进一步提高力学性能。

关键词：砖砌结构；TiNi；分层失效；轧制

(Edited by Bing YANG)